Colloid Polym Sci 278:692–696 (2000)

ORIGINAL CONTRIBUTION

O. D. Bedford
G. Ilgenfritz

Electric field effects in sodium bis(2-ethylhexyl)sulfosuccinate water-in-oil microemulsions: field-induced percolation and dynamics of structural changes

Received: 29 July 1999
Accepted: 8 February 2000

O. D. Bedford · G. Ilgenfritz
Institut für Physikalische Chemie
Universität zu Köln
Luxemburger Strasse 116
50939 Cologne, Germany
e-mails: o.bedford@uni-koeln.de
ilgenfritz@rrz.uni-koeln.de

Abstract We investigate the effect of high electric fields on the percolation behaviour of sodium bis(2-ethylhexyl)sulfosuccinate water-in-oil microemulsions in the L_2 phase and examine the existence of critical fields as a function of droplet radius and droplet concentration. It is shown that there is no direct correlation with critical fields as discussed for electrorheological fluids. Very low critical fields are found in certain ranges of droplet radii. Clustering of droplets with material exchange may be postulated under these conditions.

Key words Microemulsions · High electric fields · Percolation · Electrorheological fluids

Introduction

There are a variety of electric field effects in colloidal systems. These include the dissociation field effect of enhanced ionic dissociation of weak electrolytes, structural changes in polyelectrolytes [1], electroporation and electrofusion of cells and vesicles [2, 3], and field-induced viscosity changes in electrorheological fluids (ERFs) [4, 5]. Our research focuses on the temperature- and field-induced percolation in the macroscopic L_2 region of ionic and nonionic water-in-oil microemulsions.

In previous investigations on the nonionic Igepal system we showed [6, 7] that the temperature-induced electric percolation curve is shifted to higher temperatures at high fields and demonstrated the existence of well-defined critical fields, dependent on the distance from the percolation point.

Nonionic Igepal and ionic sodium bis(2-ethylhexyl)sulfosuccinate (AOT) microemulsions show reverse temperature dependence of the percolation transition. The first observations of field effects in AOT systems were given by Eicke and Naudts [8]. Tekle et al. [9] reported field-induced phase separation in the AOT–isooctane system.

The present article on field effects in the AOT–*n*-heptane system characterises the field effects as a function of droplet radius and droplet concentration. In particular, we focus on the existence of critical fields and examine the applicability of theoretical expressions as discussed for ERFs.

ERFs show a large increase in yield stress when subjected to an electric field above a certain critical field strength, E_c [10]. The viscosity of a microemulsion is known to rise when temperature-induced percolation takes place; accordingly, a "field-induced percolation" must also lead to a viscosity increase.

For particle interaction in ERFs it has been shown [11] that the critical field is given by

$$E_c = \sqrt{\frac{8\pi k_B T}{\alpha^2 \epsilon_m} \cdot \frac{1-\phi_{dr}}{\phi_{dr}\bar{v}}},$$
$$\alpha = \frac{(\epsilon_{dr}-\epsilon_m)}{(\epsilon_{dr}+2\epsilon_m)}, \quad (1)$$
$$\phi_{dr} = N_A c_{dr} \bar{v} \ ,$$

where ϵ_m is the dielectric constant of the oil, ϵ_{dr} is the dielectric constant of the water core, and $\bar{v}$ is the volume of one particle.

A similar expression has been applied for pearl-chain formation of cells [12]. Equation (1) arises from considering the competition between thermal and electrical energy.

The formation of conducting channels in microemulsions in the process of electric percolation requires aggregation of droplets and Eq. (1) is expected to be generally valid. It will be shown that this expression is not directly applicable to droplet microemulsions. Although microemulsions exhibit essential properties of ERFs the situation is more complex. The critical field depends strongly on the properties of the interface, which manifest themselves, for example, in the distance to the phase boundaries.

Experimental

The surfactant AOT (Sigma) was purified as described in Ref. [13]. *n*-Heptane (p.a. grade, Merck) was used as received. Water was deionized and doubly distilled. The microemulsions were prepared by weighing the components. All samples were measured within 1 week of preparation.

To describe the composition of a ternary system two variables are necessary. Here we use the molar water-to-surfactant ratio; W_0 = [water]/[AOT], and the concentration of surfactant in oil, c_{AOT}. Where appropriate we refer to the volume fraction of droplets, ϕ_{dr}, (or dispersed phase = water plus AOT) and the molar droplet concentration, c_{dr}, in the microemulsion. In all cases ideal mixing is assumed.

The percolation curves were obtained by conductivity measurements with a Tinsley Prism LCR databridge 6458 at a frequency of 1 kHz using a WTW LTA 1 electrode. A Personal computer was used for temperature control and for data acquisition from the conductivity bridge. Phase boundaries were verified by visual inspection. For the measurement of field effects we used the apparatus described in Ref. [6].

The dynamics of the electrical conductivity of the sample solution were measured with a current-viewing resistor in series with the measuring cell. In contrast to the current signal, electrobirefringence (Kerr effect) measurements allow the determination of relaxation times after the end of the field pulse. The birefringence phase shift, $\varphi = 2\pi l \Delta n/\lambda$, was calculated from the change in relative light intensity.

Results and discussion

Electric field effects were investigated as a function of droplet radius at a constant droplet concentration of 206 μM and as a function of droplet concentration at a constant radius; since the radius depends linearly on W_0 [14], a constant radius corresponds to a constant W_0; here W_0 = 35. In order to characterise the systems we determined percolation behaviour and phase boundaries.

Phase behaviour

The partial phase diagram of the water–AOT–*n*-heptane system at 25 and 40 °C can be seen in Fig. 1. As can be seen, the isotropic L_2 phase extends from the surfactant-oil side to droplet volume fractions as high as $\phi_{dr} \approx 0.7$. When starting at low surfactant concentration and increasing the water content a $\bar{2}\phi$ region is reached in which the microemulsion is in equilibrium with excess polar phase. As was pointed out early by Kunieda and Shinoda [15] and clarified by Sager [16] it is not possible to draw tie lines in the isothermic Gibbs triangle. This is due to impurities (mostly Na_2SO_4 salt).

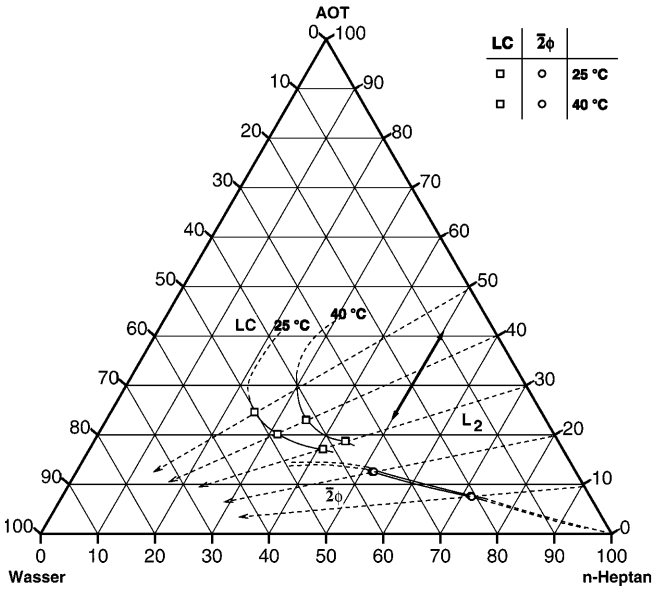

Fig. 1 Partial phase diagram for the pseudoternary water(salt)–sodium bis(2-ethylhexyl)sulfosuccinate (AOT)–*n*-heptane system at 25 and 40 °C. *LC* represents the liquid-crystalline phase

At medium surfactant concentrations and increasing water content the system separates into a liquid-crystalline phase and an L_2 phase. Between 25 and 40 °C the $\bar{2}\phi$ phase boundary does not change significantly in composition, whereas there is a noticeable change at the liquid-crystalline boundary.

Static conductivity

The results from the conductivity measurements at various compositions as a function of temperature are presented in Fig. 2. The percolation transition is characterised by an increase in conductivity of over 3 orders of magnitude. The curves can be described by scaling laws based on percolation theory [17, 18]. They can also be quite well described by a highly cooperative AB transition [7]. The results from the fits can be found in Table 1. For the determination of the exponents *s* and *t* the percolation temperature obtained from the AB fit was held fixed until the exponents reached their best (minimum χ^2) values and then, in a final step, were adjusted using the fitting algorithm. T_P did not change significantly in this last step. In all cases $t = 1.5 \pm 0.1$, a value significantly smaller than was found in previous

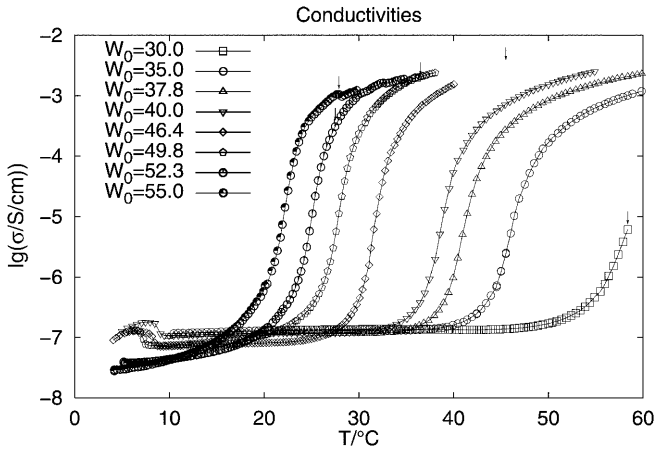

Fig. 2 Static electric conductivities as a function of temperature. Same droplet concentration, c_{dr} = 206 μM, varying droplet size (W_0) and volume fraction. Compare with Table 1. Where given the *arrows* indicate the upper phase boundaries. The other boundaries lie above 60 °C

Table 1 Composition of systems with constant droplet concentration c_{dr} = 206 μM and results from fits to the static conductivity curves. ΔH_{vH} is the van't Hoff activitation enthalpy and s and t are scaling exponents

W_0	ϕ_{dr}	AB transition		Percolation theory			
		T_P °C	ΔH_{vH} kJ/mol	T_P °C	s	T_P °C	t
30.0	0.129	59.1	414	58.3	−1.20	–	–
35.0	0.198	46.3	569	46.1	−1.20	46.3	1.47
37.8	0.233	41.2	616	40.9	−1.19	41.2	1.53
40.0	0.274	38.8	644	38.6	−1.23	38.9	1.43
46.4	0.381	31.8	738	31.8	−1.42	31.8	1.57
49.8	0.498	28.0	691	28.0	−1.51	28.0	1.56
52.3	0.572	25.1	688	25.1	−1.43	25.1	1.60
55.0	0.646	22.2	729	22.2	−1.54	22.2	1.46

investigations [18–20] and clearly lower than the theoretical predictions for dynamic percolation, $t_{th} \approx 1.9$ [21]. At low volume fractions s agrees with the theoretical value $s_{th} = -1.2$ [22], but at higher volume fractions s increases up to $s \approx 1.5$. Fits with exponents fixed to the theoretical values lead to significantly larger χ^2 values.

A possible explanation for the increase in s and the lower conductivity below percolation might be a glass transition as discussed by Sheu et al. [23].

Field experiments

For the field-pulse experiments we chose a constant temperature separation of −4 °C from the percolation point in order to separate the effects due to an external perturbation and effects due to different distances from the percolation point. Typical field experiments with simultaneous measurement of electric voltage, U, electric current, I, and birefringence phase shift, φ, at different field strengths are shown in Fig. 3.

With respect to the magnitude of conductivity three regimes can be distinguished:

1. A small current which instanteneously follows the applied electric field determined by the ohmic resistance of the cell. This current is almost negligible in Fig. 3 (0.5 mA at U = 5 kV).
2. An additional current which seems to reach its stationary value with a finite relaxation time. This can be interpreted as elongation of the clusters of droplets in the field direction.
3. A region with a field-dependent time evolution and very high conductivity which develops above a certain critical field strength, E_c.

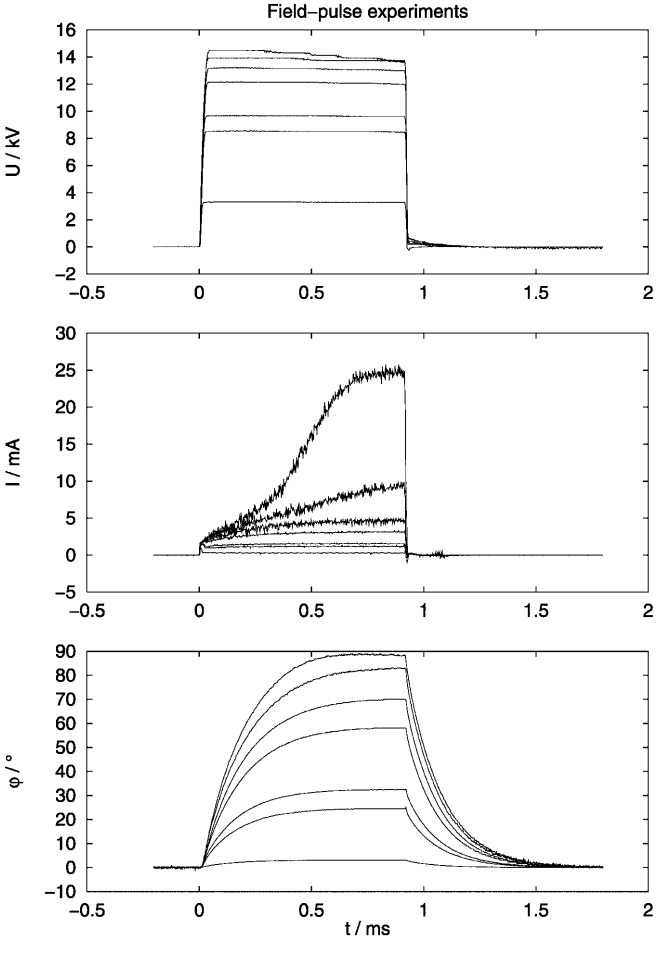

Fig. 3 Superposition of field jumps at different voltages with simultaneous measurements of phase shift and electric current. System: water–AOT–*n*-heptane, W_0 = 55

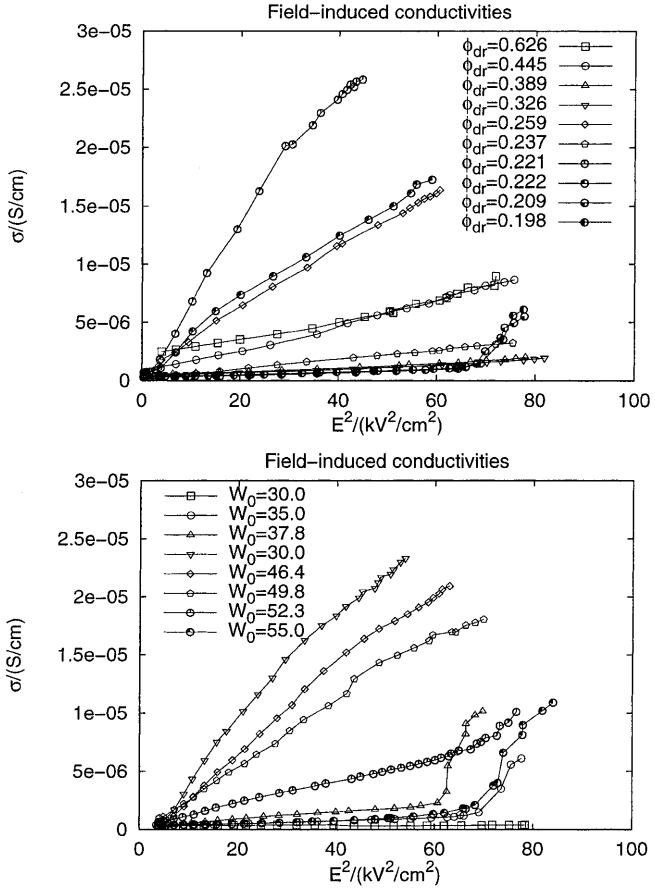

Fig. 4 **a** Conductivities as a function of field strength. Systems as in Fig 2. **b** Conductivities as a function of field strength. System: water–AOT–*n*-heptane, W_0 = 35, varying droplet concentration and volume fraction

The conductivities for the same systems as in Fig. 2 as a function of field strength can be found in Fig. 4b. Clearly not all systems exhibit a critical field strength. Besides the system at W_0 = 30, probably with an E_c exceeding the limits of our apparatus, certain systems, namely with W_0 = 40.0, 46.4, and 49.8, show a steep increase in conductivity with field strength. In the field-pulse curves (as Fig. 3) no regime 3 is observed; instead the current in regime 2 rises continuously, not reaching a plateau value but growing with time. Because of the high conductivity the field decreases and it is not possible to determine an equilibrium conductivity; therefore, all reported conductivities were calculated at a constant time (t = 0.5 ms) after the field had been applied.

The origin of the phase shift, φ, is the distortion of the water droplets resulting from the electric field. All systems, except at W_0 = 30, show a positive birefringence. The relaxation time of the field-off side increases with W_0 and ϕ_{dr}.

In the nonionic Igepal system a critical field is well established [6, 7]. As in the pioneering work of Debye and Kleboth [24] on the shift of the critical temperature by an electric field the results could be understood in terms of shifting the percolation temperature to higher values. This is not the general case in AOT systems as can be seen from Fig. 5. A shift of T_p by the electric field is not sufficient to describe the measurements.

At present we cannot give a full explanation for the factors which govern the response of an AOT microemulsion to electric fields. As was shown, there is no direct correlation with the field-free percolation point. Electric percolation is driven by aggregation of droplets into clusters and by exchange of charge carriers between droplets and clusters. The electric field affects both.

Linear aggregation is enforced by the induced dipolar interactions. The extent of induced dipolar ordering is dictated by the competition between thermal (Brownian) and electrical forces as given by Eq. (1) and was also pointed out for microemulsions by Eicke and Markovic [25, 26]. Considering only one microemulsion droplet, the induced dipolar forces are not sufficient to cause significant ordering. On the other hand, the field-induced conductivities, lying in the same range as those at the field-free percolation point, indicate the existence of extended structures. Therefore, is must be concluded that the electric field does not act on single droplets but on aggregates of droplets, which are known to exist below (in our case 4 °C) the percolation point.

The influence on the exchange rate depends crucially on the underlying mechanism. If the exchange is achieved via a fusion–fission fluctuation [27, 28] then the electric field would mainly act as a "probe" for the conductivity in the elongated clusters and no critical field would be observed. If, on the other hand, surfactant anions were "hopping" from one droplet to another [20], the necessary activation energy could

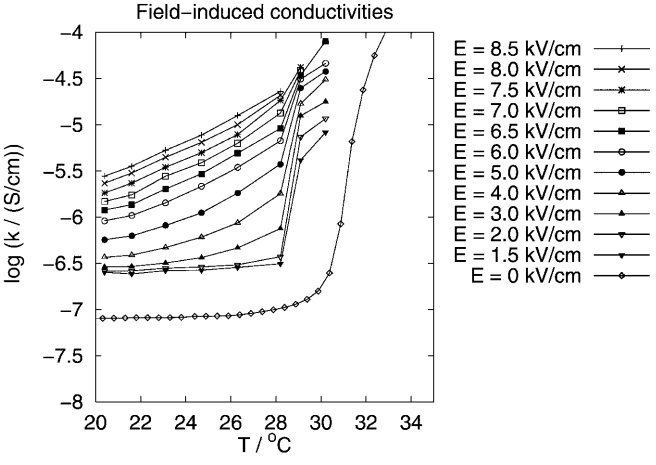

Fig. 5 Conductivities at different field strengths as a function of temperature. System: water–AOT–*n*-heptane, W_0 = 55.5, c_{AOT} = 0.2 M

drastically be changed by the field, thus resulting in a critical field. Which of these two mechanisms is realised should depend on the bending modulus or natural curvature of the interface. The curvature itself depends on temperature: a higher temperature favours a less negative curvature (towards water) as can be seen from the growing liquid–crystalline phase in Fig. 1.

It is worth noting that impurities in the AOT system (cf. Refs. [15, 16]) could also play an important role.

Conclusion

Although percolation theory gives a fair description of the temperature-induced conductivity increase, we were not able to fully describe the influence of high electric fields within this framework. In our opinion this is due to the intrinsic properties of the surfactant film, which are probed in a unique way by field-pulse experiments.

References

1. Shiga T (1997) Adv Polym Sci 134:131
2. Zimmermann U, Scheurich P, Pilwat G, Benz R (1981) Angew Chem Int Ed Engl 20:325
3. Neumann E, Kakorin S (1996) Curr Opin Colloid Interface Sci 1:790
4. Carlson JD, Sprecher AF, Conrad H (eds) (1990) Electrorheological fluids. Proceedings of the Second International Conference on Electrorheological fluids. Technomic, Lancaster
5. Tao R (ed) (1992) Electrorheological fluids: mechanism, properties, structure, technology, and applications. Proceedings of the International Conference. World Scientific, Singapore
6. Runge F, Röhl W, Ilgenfritz G (1991) Ber Bunsenges Phys Chem 95:485
7. Schlicht L, Spilgies JH, Runge F, Lipgens S, Boye S, Schübel D, Ilgenfritz G (1996) Biophys Chem 58:39
8. Eicke HF, Naudts J (1987) Chem Phys Lett 142:106
9. Tekle E, Ueda M, Schelly ZA (1989) J Phys Chem 93:5966
10. Stangroom JE (1990) In: Carlson JD, Sprecher AF, Conrad H (eds) Electrorheological fluids. Proceedings of the Second International Conference on Electrorheological fluids. Technomic, Lancaster, pp 199–206
11. Tao R (1992) In: Electrorheological fluids: mechanism, properties, structure, technology, and applications. Proceedings of the International Conference World Scientific, Singapore, pp 3–16
12. Schwan HP (1989) Dielectrophoresis and rotation of cells, Plenum, New York, pp 3–21
13. Politi MJ, Brandt O, Fendler JH (1985) J Phys Chem 89:2345
14. Fletcher PDI, Robinson BH (1981) Ber Bunsenges Phys Chem 85:863
15. Kunieda H, Shinoda K (1979) J Colloid Interface Sci 70:577
16. Sager WFC (1998) Langmuir 14:6385
17. Stauffer D, Aharony A (1995) Perkolationstheorie – eine Einführung. VCH, Weinheim
18. Chen SH, Rouch J, Sciortino F, Tartaglia P (1994) J Phys Condens Matter 6:10855
19. Cametti C, Codastefano P, Tartaglia P, Rouch J, Chen SH (1990) Phys Rev Lett 64:1461
20. Kim MW, Huang JS (1986) Phys Rev A 34:719
21. Laguës M (1979) J Phys Lett 40:L331
22. Grest GS, Webman I, Safran SA, Bug ALR (1986) Phys Rev A 33:2842
23. Sheu EY, Chen SH, Huang JS, Sung JC (1989) Phys Rev A 39:5867
24. Debye P, Kleboth K (1965) J Chem Phys 42:3155
25. Eicke HF, Markovic Z (1981) J Colloid Interface Sci 79:151
26. Eicke HF, Markovic Z (1982) J Colloid Interface Sci 85:198
27. Schelly ZA (1997) Curr Opin Colloid Interface Sci 2:37
28. Fletcher PDI, Howe AM, Robinson BH (1987) J Chem Soc Faraday Trans 1 83:985